ADAPTIVE BACKSTEPPING FRACTIONAL-ORDER NONSINGULAR TERMINAL SLIDING MODE CONTROL OF THE CONTINUOUS POLYMERIZATION REACTOR

GARBA, D. K.[1] – YAKUBU, S. O.[1] – BELLO, M. I.[2] – AHMAD, M. B.[1*]

[1] *Department of Mechanical Engineering, Nigerian Defence Academy, Kaduna, Nigeria.*

[2] *Department of Computer Science, Kano State Polytechnic, Kano State, Nigeria.*

**Corresponding author*
e-mail: mb.ahmad[at]nda.edu.ng

(Received 10th April 2024; revised 20th July 2024; accepted 31st July 2024)

Abstract. This paper proposes an adaptive backstepping fractional order nonsingular fast terminal sliding mode control (AB-FNTSMC) for a polymerization reactor subjected to model uncertainties and environmental disturbances. This controller ensures robust performance in both reaching and sliding mode phases. A fast terminal reaching law is employed to remove the chattering phenomena. An adaptation rules are used to update the upper bounds of the disturbances whose information are not required. A numerical simulation is deployed to evidence the superior performance of the AB-FNTSMC.
Keywords: *adaptive control, polymerization reactor, fractional-order, nonsingular fast terminal sliding mode control*

Introduction

In polymer chemistry, polymerization is a process in which the reacting monomers combined to form a high molecular compound (Clayden et al., 2012; Allcock et al., 1981). Polymerization reactions take place in chemical reactors (batch, semi-batch or continuous reactors) (Levenspiel, 2013) at expeditious rate and may result in explosions if not sufficiently regulated. As such, it is crucial to control the operating conditions of the reactor. The operating conditions include but not limited to monomer concentration, reaction rate, reactor temperature, coolant flow rate, initiator type (Kong and Chen, 2019; Richards and Congalidis, 2006). The contamination of measurements by sensor noises, purity of products, and variation in feed conditions and degree of mixing make polymerization reactions difficult to be controlled directly or monitored accurately (McKeen, 2014). The Automatic Continuous Online Monitoring of Polymerization reactions (ACOMP), gives the real-time measurements of the process dynamic states (McAfee et al., 2016; Kreft and Reed, 2009a; 2009b; Florenzano et al., 1998). The limitation of ACOMP is that it hardly measured the complete state vector. Therefore, an observer is required to measure all the states (Leu and Baratti, 2000). An Extended Kalman Filter (EKF) is the most commonly used measurement method in chemical industries (Salas et al., 2018; Dochain and Pauss, 1988). In Park et al. (2002), an EKF has been used to measure the states of Methyl-Methacrylate (MMA) copolymerization. In Cheng and Liu (2015), the melt index (MI) of propylene polymerization process has been estimated using least squares support vector machine. In Kupilik and Vincent (2011), an EKF has been applied to measure the biogas composition in a Continuous Stirred Tank Reactor (CSTR). A hierarchical EKF has been used to estimate the kinetic parameters in the production of ethylene-propylenediene polymer (Li et al., 2004).

In order to compensate the uncertainties and external disturbances deteriorating the operations of chemical processes, sliding mode control (SMC) strategies are employed. In Sinha and Mishra (2018), an event driven SMC was proposed for a chemical reactor. A Sliding mode observer based control has been implemented in Aguilar-López amd Maya-Yescas (2005) for a fermentation process and in Rahman et al. (2010) for a batch polymerization reactor. In Narwekar and Shah (2020), a SMC was suggested for temperature control of a batch process. In Kadu et al. (2018), a decentralised SMC was developed for the control of two-input-two-output chemical reactor. A temperature trajectory tracking SMC has been designed for a batch reactor (Chen, 2012). The time-varying Parameters in chemical processes add more difficulties to the control design. An adaptive SMC based support vector machine was designed for a chemical reactor in Uçak and Öke Günel (2020). In Wu et al. (2017), a model free adaptive controller has been constructed to control molecular weight distribution in styrene polymerization. In Yuan et al. (2017), an adaptive control technique was implemented for a nonlinear wiener model and it was applied for composition control in a chemical reactor. Nonetheless, adaptive control schemes are limited to systems with constant or slow time varying parameters. This limitation can be lifted by deploying neural network (NN) to approximate the system dynamics. A NN based MPC was used for temperature control of a multi-product batch reactor (Kamesh and Rani, 2016). A RBFNN based internal model controller was utilised to control the average molecular weight in the free radical polymerization of MMA. A NN based generic model control was developed for a multivariable semi-batch reactor (Kamesh and Rani, 2017).

Considering the foregoing discussion, in this paper, we integrate backstepping, fractional order nonsingular terminal sliding mode surface, and adaptive reaching laws to control the monomer concentration and the temperature of a polymerization reactor with uncertain dynamics. Furthermore, this is the first time a ABFNTSMC is proposed to control the reactor. The main contributions of this article include: (1) In order to improve the robustness against disturbances, a FNTSM surface has been proposed. Moreover, by combining the FNTSMC with backstepping, the tracking accuracy is greatly enhanced; (2) In Narwekar and Shah (2020), Kadu et al. (2018), Sinha and Mishra (2018), Chen (2012), Rahman et al. (2010), as well as Aguilar-López and Maya-Yescas (2005), the upper bounds of the disturbances are known. However, chemical processes have multiple operating points and therefore it is difficult to obtain the upper bounds of the dynamic disturbances at each operating region. As a result, we used adaptive laws to estimate the upper bounds of the disturbances. In addition, fast terminal reaching laws are utilised to do away with chattering effects; (3) A Lyapunov candidate function is used to show the convergence and the stability of the closed loop system.

Mathematical model

We consider the free radical polymerization of styrene monomers initiated by azobis-iso-butyronitrile dissolved in a pure benzene in a jacketed continuous stirred tank reactor depicted in *Figure 1*. The heat released by the exothermic process is removed by a cooling jacket using water as the cooling fluid. The dynamic model of the reactor is derived from material and energy balance equations as (Biswas and Samanta, 2013).

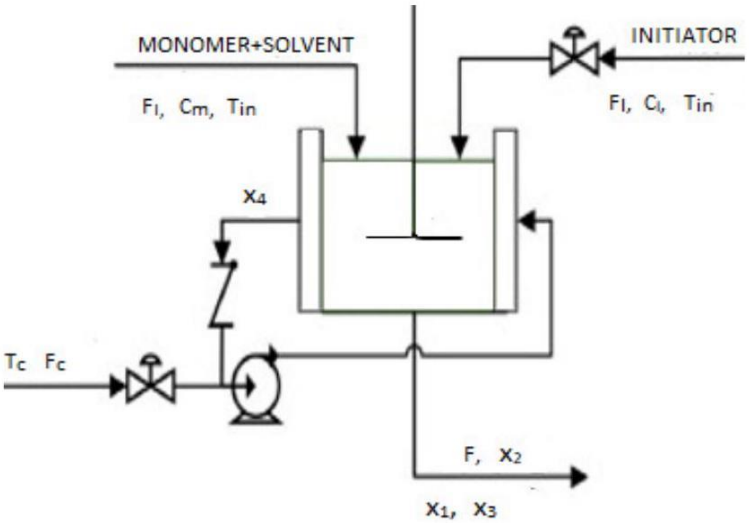

Figure 1. *A simple schematic diagram of the polymerization reactor.*

$$\dot{x}_1 = -(k_p + k_{fm})\zeta_0 x_1 + \frac{F_m(C_m - x_1)}{v} \quad \text{Eq. (1)}$$

$$\dot{x}_2 = -k_I x_2 + \frac{F_i C_I - F x_2}{v} \quad \text{Eq. (2)}$$

$$\dot{x}_3 = k_p \frac{(-\Delta H_p)}{\rho c_p} x_1 \zeta_0 - \frac{UA}{\rho c_p v}(x_3 - x_4) + \frac{F(T_{in} - x_3)}{v} \quad \text{Eq. (3)}$$

$$\dot{x}_4 = \frac{F_c T_c - F x_4}{v_c} + \frac{UA}{\rho_c c_c v_c}(x_3 - x_4); \zeta_0 = \left[\frac{2 f k_I}{k_{Tc} + k_{Td}}\right]^{1/2} \sqrt{x_2} \quad \text{Eq. (4)}$$

$$M = x_1;\ T = x_3. \quad \text{Eq. (5)}$$

where $x_1(\text{kmol/m}^3), x_2(\text{kmol/m}^3)$ denote the monomer and the initiator concentrations respectively, $x_3(^0K)$ and $x_4(^0K)$ stand for the reactor and the coolant's temperatures respectively. The outputs are $M = x_1$ and $T = x_3$. The inputs are the coolant flow rate $F_c\ m^3/h$ and the initiator flow rate $F_i m^3/h$. The definition and the values of the reactor parameters are given in *Table 1*.

Table 1*. The definitions and values of the reactor parameters.*

Symbols	Values	Meaning
v	$1.0m^3$	Reactor volume
T	$335K$	Reactor temperature
F	$10.0m^3/h$	Monomer flow rate
f^*	0.58	Initiator efficiency
k_p	2.50×10^6 m^3/(kmol. h)	Propagation rate constant
k_{Tc}	1.33×10^{10} m^3/(kmol. h)	Termination by coupling rate constant
k_{Td}	1.09×10^{11} m^3/(kmol. h)	Termination by disproportionation rate constant
C_m	6.00kmol/m^3	Inlet monomer concentration
C_I	8.00kmol/m^3	Inlet monomer concentration
K_I	$1.02 \times 10^{-1} h^{-1}$	Initiation rate constant
$k_{fm\ rl}$	2.45×10^3 m^3/(kmol. h)	Chain transfer to monomer rate constant
M_m	100.12 kg/kmol	Molecular weight of the monomer

ρ	$866 kgm^3$	Density of the reacting mixture
$\rho_{c\ r}\ r_1$	$1000\ kg.m^3$	Density of water
c_p	$2.0\ kJ_1 kg^{-1} \cdot K^{-1}$	Heat capacity of the reacting mixture
$-\Delta H_p$	$57800 kJ.kmol^{-1}$	Heat of propagation reaction
U	$720 kJ.h^{-1} \cdot K^{-1}$	Overall heat transfer coefficient
A	$2.0 m^2$	Heat transfer area
c_c	$4.2 kj.kg^{-1}.K^{-1}$	Heat capacity of water
T_{in}	$350K$	Temperature of the inlet streams in the reactor
T_c	$293.2K$	Temperature of the inlet coolant stream

Preliminaries

The general definition of the fractionalorder derivative and integration is given by Chen et al. (2019):

$$ {}_{\theta}\mathcal{D}_t^{\mu} = \begin{cases} \dfrac{d^{\mu}}{dt^{\mu}} & \mathrm{Re}(\mu) > 0. \\ 1 & \mathrm{Re}(\mu) = 0. \\ \int_{\theta}^{t} d\tau^{\mu} & \mathrm{Re}(\mu) < 0. \end{cases} \qquad \text{Eq. (6)} $$

where $\mathcal{D}$ is the fractional calculus operator, μ represents the fractional order which can be complex or real, θ and t stand for the lower and upper limits of the operation, $\mathrm{Re}(\mu)$ represents the real part μ. The Riemann-Liouville definition of the fractional-order calculus is given by:

$$ {}_{\theta}\mathcal{D}_t^{\mu} = \left(\frac{d}{dt}\right)^n \frac{1}{\Gamma(n-\mu)} \int_{\theta}^{t} \frac{f(\tau)}{(t-\tau)^{\mu-n+1}} \qquad \text{Eq. (7)} $$

$n-1 < \mu < n, n \in \mathcal{N}, \mu \in \mathcal{R}$ and $\Gamma(.) isagamma$ function. Assumption 1 The disturbances are bounded $\Delta_i \leq K_i (i = m, T)$; by differentiating M and T from (5) with respect to time, we have:

$$ \begin{cases} \dot{M} = \dfrac{\partial M}{\partial x_1} \dot{1} + \dfrac{\partial M}{\partial x_2} \dot{x_2}. \\ \dot{T} = \dfrac{\partial T}{\partial x_1} \dot{x_1} + \dfrac{\partial T}{\partial x_2} \dot{x_2} + \dfrac{\partial T}{\partial x_3} \dot{x_3} + \dfrac{\partial T}{\partial x_4} \dot{x_4}. \end{cases} \qquad \text{Eq. (8)} $$

Differentiating (8) with respect to time yields:

$$ \begin{cases} \ddot{M} = \dfrac{\partial(\dot{M})}{\partial x_1)} \dot{x}_1 + \dfrac{\partial(\dot{M})}{\partial x_2} \dot{x}_2. \\ \ddot{T} = \dfrac{\partial(\bar{T})}{\partial x_1} \dot{x}_1 + \dfrac{\partial(\dot{T})}{\partial x_2} \dot{x}_2 + \dfrac{\partial(\dot{T})}{\partial x_3} \dot{x}_3 + \dfrac{\partial(\dot{T})}{\partial x_4} \dot{x}_4. \end{cases} \qquad \text{Eq. (9)} $$

It is obvious that the inputs can be extracted from Eq. (9). Therefore:

$$ \begin{cases} \ddot{M} = A_1(x) + B_{11}(x) F_i. \\ \ddot{T} = A_2(x) + B_{21}(x) F_i + B_{22}(x) F_c. \end{cases} \qquad \text{Eq. (10)} $$

Where;

$$A_1(x) = \frac{\partial(\dot{M})}{\partial x_1}\dot{x}_1 + \frac{\partial(\dot{M})}{\partial x_2}\left[-k_I x_2 + \frac{-Fx_2}{v}\right]$$

$$A_2(x) = \frac{\partial(\dot{T})}{\partial x_1}\dot{x}_1 + \frac{\partial(\dot{T})}{\partial x_2}\left[-k_I x_2 + \frac{-Fx_2}{v}\right] + \frac{\partial(\dot{T})}{\partial x_3}\dot{x}_3 + \frac{\partial(\dot{T})}{\partial x_4}\left[\frac{-Fx_4}{v_c} + \frac{UA(x_3 - x_4)}{\rho_c c_c v_c}\right]$$

$$B_{11}(x) = \frac{C_I}{v}\frac{\partial(\dot{M})}{\partial x_2},\ B_{21}(x) = \frac{\partial(\dot{T})}{\partial x_2}\frac{C_I}{v}$$

$$B_{22}(x) = \frac{\partial(\dot{T})}{\partial x_4}\frac{T_c}{v_c},\ U_1 = F_i,\ U_2 = F_c$$

From Eq. (10), we have:

$$\begin{cases}\dot{\xi}_1 &= \xi_2 \\ \dot{\xi}_2 &= A(x) + B(x)U + \Delta\end{cases} \#.(11) \qquad \text{Eq. (11)}$$

Where;

$$\xi_1 = \begin{bmatrix}M_1 \\ T_1\end{bmatrix},\ \xi_2 = \begin{bmatrix}M_2 \\ T_2\end{bmatrix},\ A(x) = \begin{bmatrix}A_1(x) \\ A_2(x)\end{bmatrix},$$

$$U = \begin{bmatrix}U_1 \\ U_2\end{bmatrix},\ \Delta = \begin{bmatrix}\Delta_1 \\ \Delta_2\end{bmatrix},\ B(x) = \begin{bmatrix}B_{11}(x) & 0 \\ B_{21}(x) & B_{22}(x)\end{bmatrix}$$

where Δ denotes the external disturbances. $B^{-1}(x)$ exists since $\det(B(x)) = B_1(x)B_2(x) \neq 0$.

Control design

In this section, the proposed AB-FNTSMC is dveloped for the control of monomer concentration and reactor temperature. In addition, a robust backstepping with integral sliding mode controller (RBISMC) and feedback linearization controller (FLC) are designed for comparison with the AB-FNTSMC.

Design of AB-FNTSMC

The tracking errors are expressed as:

$$z_1 = \xi_1 - \xi_d;\ \dot{z}_1 = \dot{\xi}_1 - \dot{\xi}_d = \xi_2 - \dot{\xi}_d$$

$$z_2 = \xi_2 - \dot{\xi}_d;\ \dot{z}_2 = \dot{\xi}_2 - \ddot{\xi}_d$$

where $z_1 = [z_m \quad z_T]^T, z_2 = [\dot{z}_m \quad \dot{z}_T]^T$ are the vectors of tracking errors and $\xi_d = [M_d \quad T_d]^T$ is the vector of the desired trajectories. The FNTSM surface is specified as Wang et al. (2019).

$$S = z_2 + \Lambda_1 D^{\mu_1}[\text{sign}(z_1)^p] + \Lambda_2 D^{\mu_2 - 1}[\text{sign}(z_1)^q \quad \text{Eq. (12)}$$

Where;

$$S = \begin{bmatrix} S_M \\ S_T \end{bmatrix};\ \Lambda_1 = \begin{bmatrix} \Lambda_{1m} & 0 \\ 0 & \Lambda_{1T} \end{bmatrix};\ \Lambda_2 = \begin{bmatrix} \Lambda_{2m} & 0 \\ 0 & \Lambda_{2T} \end{bmatrix}$$

$$\text{sign}(z_1)^p = \begin{bmatrix} \text{sign}(z_m)^p \\ \text{sign}(z_T) \end{bmatrix} : \text{sign}(z_1)^q = \begin{bmatrix} \text{sign}(z_m)^q \\ \text{sign}(z_T)^q \end{bmatrix}$$

The time derivative of the sliding surface Eq. (12) yields:

$$\begin{aligned} \dot{S} &= \dot{z}_2 + \Lambda_1 D^{\mu+1}[\text{sign}(z_1)^p] + \Lambda_2 D^{\mu_2}[\text{sign}(z_1)^q] \\ &= \dot{\xi}_2 - \ddot{\xi}_d + \Lambda_1 D^{\mu+1}[\text{sign}(z_1)^p] + \Lambda_2 D^{\mu_2}[\text{sign}(z_1)^q] \\ &= A(x) + B(x)U + \Delta - \ddot{\xi}_d + \Lambda_1 D^{\mu+1}[\text{sign}(z_1)^p] \end{aligned} \quad \text{Eq. (13)}$$

Select a Lyapunov function as:

$$L_1 = \frac{1}{2} z_1^T z_1 \quad \text{Eq. (14)}$$

$$\dot{L}_1 = z_1^T \dot{z}_1 = z_1^T (\dot{\xi}_1 - \dot{\xi}_d) = z_1^T (\xi_2 - \dot{\xi}_d) \quad \text{Eq. (15)}$$

The virtual controller is designed as;

$$\xi_2 = \dot{\xi}_d - C z_1 - S \quad \text{Eq. (16)}$$

where $C = C^T > 0$ is a constant diagonal matrix. Inserting the virtual input Eq. (16) into Eq. (14) gives;

$$\dot{L}_1 = -z_1^T C z_1 + z_1^T S \quad \text{Eq. (17)}$$

Consider the following Lyapunov function:

$$L_2 = \frac{1}{2} z_1^T z_1 + \frac{1}{2} S^T S \quad \text{Eq. (18)}$$

Differentiating Eq. (18) with respect to time, we have;

$$\dot{L}_2 = z_1^T \dot{z}_1 + S^T \dot{S} = -z_1^T C z_1 + S^T (z_1 + \dot{S}) \quad \text{Eq. (19)}$$

Where;

$$r = -\ddot{\xi}_d + \Lambda_1 D^{\mu+1}[\text{sign}(z_1)^p] + \Lambda_2 D^{\mu_2}[\text{sign}(z_1)^q]$$

To guarantee fast convergence and excellent tracking accuracy with the existence of model perturbations and disturbances, a FTSM reaching law is developed as:

$$\dot{S} = -B(x)^{-1}\left[R_1 S + R_2 \text{sign}(S)^{\vartheta}\right] \quad \text{Eq. (20)}$$

where $\text{sign}(S)^{\vartheta} = \left[\text{sign}(S_M)^{\vartheta}, \text{sign}(S_T)^{\vartheta}\right]^T, R_1$ and R_2 are unknown constant diagonal matrices. Therefore, the robust controller can be written as:

$$U = B^{-1}(x)\left[-z_1 - A(x) - r - \hat{R}_1 S - \hat{R}_2 \text{sign}(S)^{\vartheta}\right] \quad \text{Eq. (21)}$$

where $\hat{R}_i$ is the estimate matrices $\hat{R}_i (\text{i} = 1,2)$. The matrices are estimated by the following adaptation laws:

$$\begin{cases} \dot{\hat{R}}_1 = \alpha_1\left[\text{diag}(S)^T \text{diag}(S) - \kappa_1 \hat{R}_1\right]. \\ \dot{\hat{R}}_2 = \alpha_2\left[\text{diag}(S)^T \text{diag}(\text{sign}(S))^{\vartheta} - \kappa_1 \hat{R}_2 \cdot\right] \end{cases} \quad \text{Eq. (22)}$$

where $\alpha_1 = \alpha_1^T > 0, \alpha_2 = \alpha_2^T > 0$ are constant diagonal matrices, $\kappa_1 > 0, \kappa_2 > 0$ are small constants.

Theorem 1

For the input-output dynamics Eq. (11) under the FNFTSM surface Eq. (12), if the adaptive control law is established as Eq. (21) updated with Eq. (22), then, S, z_1, z_2, $\tilde{R}_1$, and $\tilde{R}_2$ are ultimately uniformly bounded. Proof By augmenting the Lyapunov function Eq. (18), we get:

$$L_2 = \frac{1}{2} z_1^T z_1 + \frac{1}{2} S^T S + \frac{1}{2} \tilde{R}_1^T \alpha_1^{-1} \tilde{R}_1 + \frac{1}{2} \tilde{R}_2^T \alpha_2^{-1} \tilde{R}_2 \quad \text{Eq. (23)}$$

Differentiating (23) with respect to time, we have:

$$\begin{aligned} \dot{L}_2 &= z_1^T \dot{z}_1 + S^T \dot{S} + \tilde{R}_1^T \alpha_1^{-1} \dot{\tilde{R}}_1 + \tilde{R}_2^T \alpha_2^{-1} \dot{\tilde{R}}_2 \\ &= -z_1^T C z_1 + S^T (z_1 + A(x) + B(x)U + \Delta + r) \end{aligned} \quad \text{Eq. (24)}$$

Substituting the control input Eq. (21) into Eq. (24), one has:

$$\dot{L}_2 = -z_1^T C z_1 + S^T\left(\Delta - \hat{R}_1 S - \hat{R}_2 \text{sign}(S)^{\vartheta}\right) \quad \text{Eq. (25)}$$

Noting that $\hat{R}_i = R_i - \tilde{R}_i (\text{i} = 1,2)$, we achieve:

$$\begin{aligned} \dot{L}_2 &= -z_1^T C z_1 + S^T\left(\Delta - R_1 S - R_2 \text{sign}(S)^{\vartheta}\right) \\ &\quad + \tilde{R}_1\left[\text{diag}(S)^T \text{diag}(S) - \alpha_1^{-1} \dot{\hat{R}}_1\right] \end{aligned} \quad \text{Eq. (26)}$$

Substituting the update laws Eq. (22) into Eq. (26) yields:

$$\dot{L}_2 = -z_1^T C z_1 - S^T R_1 S + S^T R_0 \text{sign}(S)^{\vartheta} \quad \text{Eq. (27)}$$

where $R_0 = \left[\text{diag}(\Delta)\text{diag}^{-1}\left(\text{sign}(S)^{\vartheta}\right) - R_2\right]$. Using the following Young's inequalities;

$$\tilde{R}_i\hat{R}_i = \tilde{R}_i\left[R_i - \tilde{R}_i\right] \leq \frac{\|R_i\|^2}{2} - \frac{\|\tilde{R}_i\|^2}{2} (i = 1,2)$$
$$S^T R_1 S \leq \| S \|^2 \|R_1\|; S^T R_0 \text{sign}(S)^{\vartheta} \leq \| S \|^{1+\vartheta} \|R_0\|;$$
$$\| S \|^{2(1+\vartheta)} \|R_0\|^2 \leq \| S \|^2 \|R_0\|^2, \| S \|^2 \to 0$$

Equation (27) can be written as:

$$\dot{L} \leq -m\left[\frac{\|z_1\|^2}{2} + \frac{\| S \|^2}{2} + \frac{\|\tilde{R}_1\|^2}{2\|\alpha_1\|} + \frac{\|\tilde{R}_2\|^2}{2\|\alpha_2\|}\right] + \frac{\|R_1\|^2}{2} + \frac{\|R_2\|^2}{2} \quad \text{Eq. (28)}$$

Therefore,

$$L \leq -mL + n \quad \text{Eq. (29)}$$

where $m = \min\{\| C \|, 2(\|R_1\| - \|R_3\|)\kappa\|\alpha_1\|, \kappa\|\alpha_2\|, n = \frac{\|R_1\|^2}{2} + \frac{\|R_2\|^2}{2}$. Integrating (38) yields;

$$L \leq \frac{n}{m} + L(0)e^{-mt} \quad \text{Eq. (30)}$$

As $t \to \infty, L \leq \frac{n}{m}$. Therefore, the closed loop signals are uniformly ultimately bounded in the compact set $\beta = \left\{L: L \leq \frac{n}{m}\right\}$

Design of RBISMC

The ISMC surface is defined as Ullah et al. (2020):

$$S = z_2 + \Pi_1 \int z_1 dt. \quad \text{Eq. (31)}$$

where $\Pi_1 = \Pi_1^T > 0$ is a constant diagonal matrices. The fictitious controller is designed as:

$$\xi_2 = \dot{\xi}_d - C_2 z_1 - S \quad \text{Eq. (32)}$$

where $C_2 = C_2^T > 0$ is a diagonal matrix. The control input is developed as:

$$\begin{cases} U = U_{eq} + U_r. \\ U_{eq} = B^{-1}(x)\left[-A(x) + \ddot{\xi}_d - z_1 - \Pi_1 z_1\right]. \\ U_r = -B^{-1}(x)R_3\text{sign}(S). \end{cases} \quad \text{Eq. (33)}$$

where $R_3 = R_3^T > 0$ is a diagonal matrix.

Theorem 2

For the input-output dynamics Eq. (10) controlled by Eq. (32) and Eq. (33) under the ISM surface Eq. (31), then the system is asymptotically stable. Proof We consider the Lyapunov function:

$$L_3 = \frac{1}{2} z_1^T z_1 + \frac{1}{2} S^T S \qquad \text{Eq. (34)}$$

By computing the time-derivative of Eq. (34), one gets:

$$\dot{L}_3 = z_1^T \dot{z}_1 + S^T \dot{S} = z_1^T \left(\xi_2 - \dot{\xi}_d\right) + S^T \left(A(x) + B(x)U + \Delta - \ddot{\xi}_d + + \Pi_1 z_1\right) \qquad \text{Eq. (35)}$$

Using the virtual controller Eq. (32), one has:

$$\dot{L}_3 = -z_1^T C_2 z_1 + S^T [z_1 + A(x) + B(x)U + \Delta \qquad \text{Eq. (36)}$$

From the control law Eq. (33), Eq. (36) becomes:

$$\begin{aligned} \dot{L}_3 &= -z_1^T C_2 z_1 + S^T [\Delta - R_3 \text{sign}(S)] \\ &\leq -\|C_2\| \|z_1\|^2 - \| S \| [\|R_3 - \text{diag}(\Delta)\|] \end{aligned} \qquad \text{Eq. (37)}$$

Where $\tilde{R}_3 = R_3 - \text{diag}(\Delta) > 0$.

Design of FLC

Equation (10) can be rewritten as:

$$\begin{bmatrix} \ddot{M} \\ \ddot{T} \end{bmatrix} = \begin{bmatrix} A_1(x) \\ A_2(x) \end{bmatrix} + \begin{bmatrix} B_{11}(x) & 0 \\ B_{21}(x) & B_{22}(x) \end{bmatrix} \begin{bmatrix} U_1 \\ U_2 \end{bmatrix} \qquad \text{Eq. (38)}$$

The global feedback linearization input is thus:

$$U = \begin{bmatrix} U_1 \\ U_2 \end{bmatrix} = - \begin{bmatrix} B_{11}(x) & 0 \\ B_{21}(x) & B_{22}(x) \end{bmatrix}^{-1} \begin{bmatrix} A_1(x) \\ A_2(x) \end{bmatrix} + \begin{bmatrix} \Omega_1 \\ \Omega_2 \end{bmatrix} \qquad \text{Eq. (39)}$$

where $\Omega_i (\text{i} = 1,2)$ are auxiliary inputs. If $A_i(x), B_i(x)$ $(\text{i} = 1,2)$ are completely available, using (39), (38) becomes:

$$\begin{cases} \ddot{M} = \Omega_1. \\ \ddot{T} = \Omega_2. \end{cases} \qquad \text{Eq. (40)}$$

Then, the linearized system is thus:

$$\begin{bmatrix} \dot{M}_1 \\ \dot{M}_2 \\ \dot{T}_1 \\ \dot{T}_2 \end{bmatrix} = \begin{bmatrix} 0 & 1 & 0 & 0 \\ 0 & 0 & 0 & 0 \\ 0 & 0 & 0 & 1 \\ 0 & 0 & 0 & 0 \end{bmatrix} \begin{bmatrix} M_1 \\ M_2 \\ T_1 \\ T_2 \end{bmatrix} + \begin{bmatrix} 0 & 0 \\ 1 & 0 \\ 0 & 0 \\ 0 & 1 \end{bmatrix} \begin{bmatrix} \Omega_1 \\ \Omega_2 \end{bmatrix}. \quad \text{Eq. (41)}$$

Therefore, the auxiliary controller is chosen as:

$$\begin{cases} \Omega_1 = \ddot{M}_d + R_{pM} z_M + R_{iM} \int z_M dt + R_{dM} \dfrac{dz_M}{dt}. \\ \Omega_2 = \ddot{T}_d + R_{pT} z_T + R_{iT} \int z_T dt + R_{dT} \dfrac{dz_T}{dt}. \end{cases} \quad \text{Eq. (42)}$$

Where R_{pj}, R_{ij}, and $R_{dj} (j = M, T)$ are the proportional, integral and derivative gains.

Results and Discussion

In this section, simulation results are provided to show the satisfactory performance of the AB-FNTSMC designed. In addition, the Proposed AB-FNTSMC is compared with RBISMC and FLC. The parameters of the reactor are given in Table 1. The states of the process are simulated with an initial value of $x_i(0) = 0.001$ (i = 1,2,3,4). A model uncertainty of 30% and external disturbances $\Delta_1 = 2, \Delta_2 = 18$ have been considered in the simulation. The parameters of the controllers are provided in *Table 2*. The simulation results for the polymerization reactor control are presented in *Figure 2* to *Figure 6*. As shown in *Figure 2*, the FLC failed to trace the reference trajectories in the presence of dynamic uncertainties. Due to the robustness of the RBISMC, it is able compensate the uncertainties and track the reference signals. The responses of the outputs under the AB-FNTSMC are superior compared to both FLC and RBISMC due to its adaptive nature and robustness of the FNTSM surface. The tracking errors depicted in *Figure 3* converge to zero at a quicker rate under the AB-FNTSMC. The control signals of the AB-FNTSMC have no chattering unlike the RBISMC as shown in *Figure 4*. The evolution of the parameters of reaching laws are shown in *Figure 5* and *Figure 6*.

***Table 2**. The control parameters.*

Controllers	Values
AB-FNTSMC	$\Lambda_1 = \text{diag}(2.4,3.7), \Lambda_2 = \text{diag}(1.1,2.6)$ $\mu_1 = \mu_2 = 0.9, \text{p} = 0.5, \text{q} = 1.5$ $\text{C} = \text{diag}(13,22)$ $\alpha_1 = \text{diag}(0.05,0.01), \alpha_2 = \text{diag}(0.9,4)$
RBISMC	$\Pi_1 = \text{diag}(18,30), C_2 = \text{diag}(8,15)$ $R_3 = \text{diag}(12,16)$
FLC	$R_{pM} = 21, R_{dM} = 13, R_{iM} = 3$ $R_{pT} = 14, R_{dT} = 9, R_{iT} = 1.6$

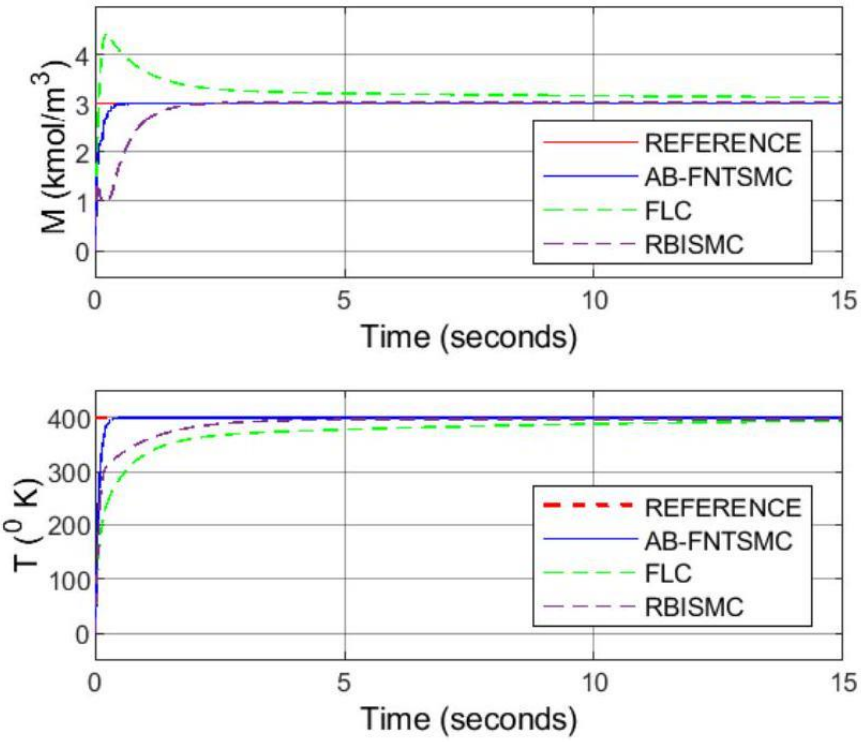

Figure 2. *Outputs' tracking.*

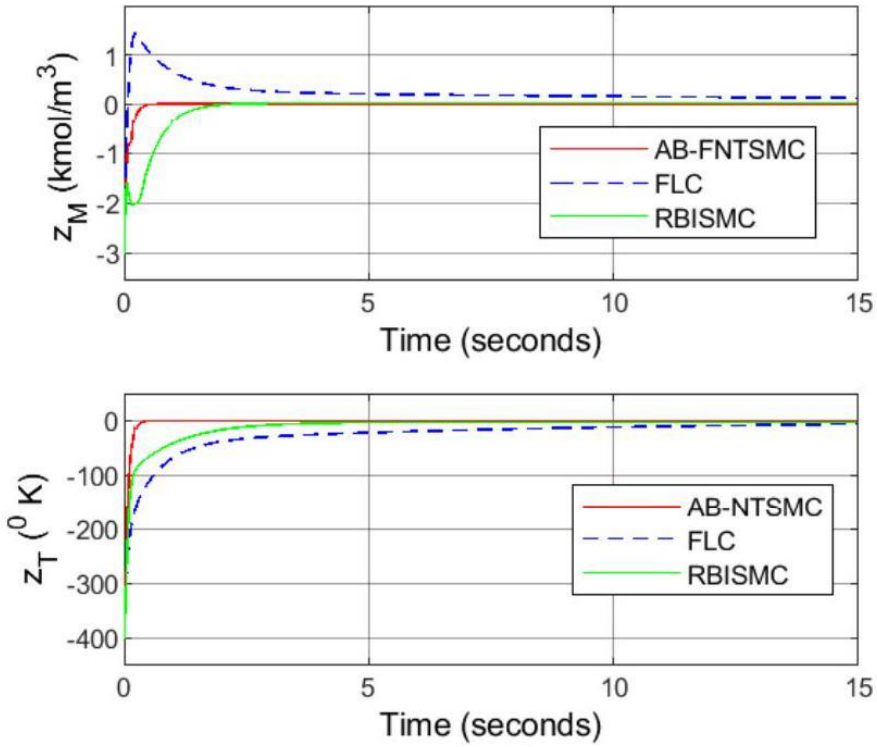

Figure 3. *Position tracking result.*

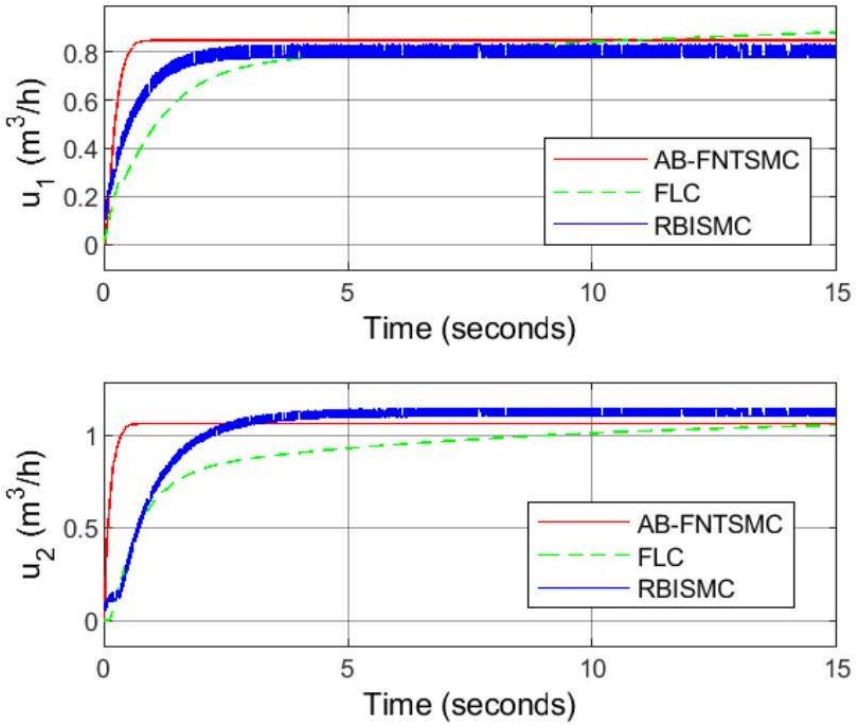

Figure 4. *The control inputs.*

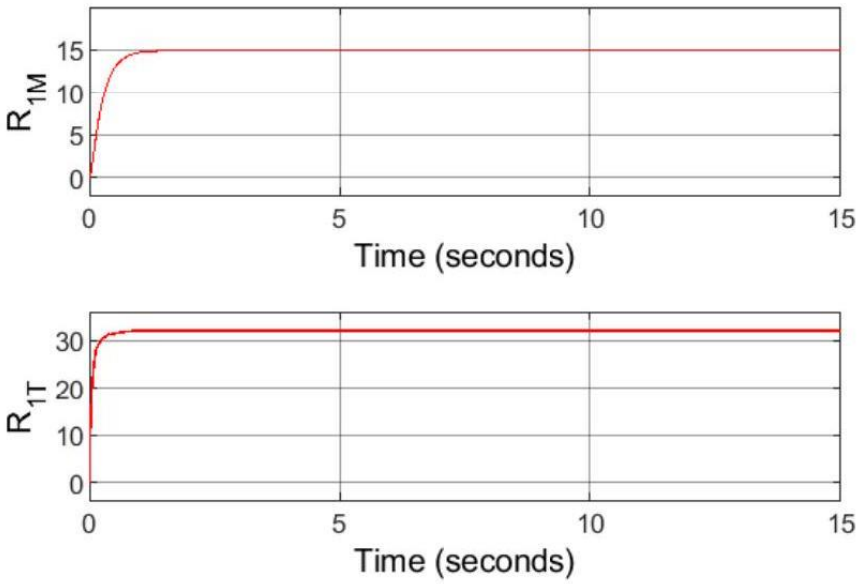

Figure 5. *Elements of the matrix* R_1.

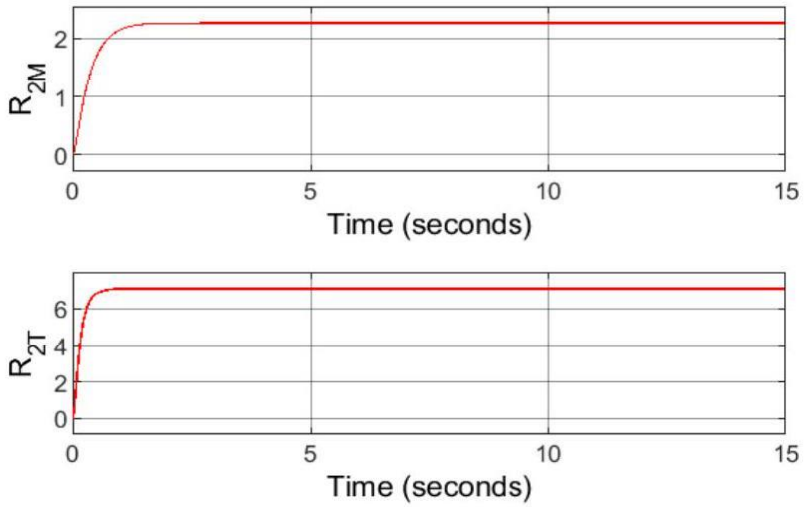

Figure 6. *Elements of the matrix* R_2.

Conclusion

A robust AB-FNTSMC scheme for an uncertain polymerization reactor is developed in this article. The proposed controller admits strong robustness against external disturbances and uncertain model parameters. The chattering phenomena have been eliminated with the aid of fast terminal reaching laws with adaptive gains. Finally, some simulations have been executed to illustrate the efficiency of the devised method compared to FLC and RBISMC.

Acknowledgement

This research is self-funded.

Conflict of interest

The authors confirm that there is no conflict of interest involve with any parties in this research study.

REFERENCES

[1] Aguilar-López, R., Maya-Yescas, R. (2005): State estimation for nonlinear systems under model uncertainties: a class of sliding-mode observers. – Journal of Process Control 15(3): 363-370.

[2] Allcock, H.R., Lampe, F.W., Mark, J.E., Allcock, H.R. (1981): Contemporary polymer chemistry. – Englewood Cliffs, NJ: Prentice-Hall 3p.

[3] Biswas, P., Samanta, A.N. (2013): Backstepping control of polymerization reactor. – In 2013 9th Asian Control Conference (ascc), IEEE 5p.

[4] Chen, C.T. (2012): A sliding mode control strategy for temperature trajectory tracking in batch processes. – IFAC Proceedings Volumes 45(15): 644-649.

[5] Chen, S.Y., Chiang, H.H., Liu, T.S., Chang, C.H. (2019): Precision motion control of permanent magnet linear synchronous motors using adaptive fuzzy fractional-order sliding-mode control. – IEEE/ASME Transactions on Mechatronics 24(2): 741-752.

[6] Cheng, Z., Liu, X. (2015): Optimal online soft sensor for product quality monitoring in propylene polymerization process. – Neurocomputing 149: 1216-1224.
[7] Clayden, J., Greeves, N., Warren, S. (2012): Organic chemistry. – Oxford University Press, USA 1260p.
[8] Dochain, D., Pauss, A. (1988): On-line estimation of microbial specific growth-rates: An illustrative case study. – The Canadian Journal of Chemical Engineering 66(4): 626-631.
[9] Florenzano, F.H., Strelitzki, R., Reed, W.F. (1998): Absolute, on-line monitoring of molar mass during polymerization reactions. – Macromolecules 31(21): 7226-7238.
[10] Kadu, C.B., Khandekar, A.A., Patil, C.Y. (2018): Sliding mode controller with state observer for TITO systems with time delay. – International Journal of Dynamics and Control 6: 799-808.
[11] Kamesh, R., Rani, K.Y. (2017): Application of artificial neural network-based generic model control to multivariable processes. – Asia-Pacific Journal of Chemical Engineering 12(5): 775-789.
[12] Kamesh, R., Rani, K.Y. (2016): Novel formulation of adaptive MPC as EKF using ANN model: Multiproduct semibatch polymerization reactor case study. – IEEE Transactions on Neural Networks and Learning Systems 28(12): 3061-3073.
[13] Kong, J., Chen, X. (2019): Dynamic optimization of batch free radical polymerization with conditional modeling formulation through the adaptive smoothing strategy. – Computers & Chemical Engineering 120: 15-29.
[14] Kreft, T., Reed, W.F. (2009a): Predictive control and verification of conversion kinetics and polymer molecular weight in semi-batch free radical homopolymer reactions. – European Polymer Journal 45(8): 2288-2303.
[15] Kreft, T., Reed, W.F. (2009b): Predictive control of average composition and molecular weight distributions in semibatch free radical copolymerization reactions. – Macromolecules 42(15): 5558-5565.
[16] Kupilik, M.J., Vincent, T.L. (2011): Estimation of biogas composition in a catalytic reactor via an extended Kalman filter. – In 2011 IEEE international conference on control applications (CCA), IEEE 6p.
[17] Levenspiel, O. (2013). Chemical Reactor Omnibook-soft cover. – Lulu Publisher 730p.
[18] Leu, G., Baratti, R. (2000): An extended Kalman filtering approach with a criterion to set its tuning parameters; application to a catalytic reactor. – Computers & Chemical Engineering 23(11-12): 1839-1849.
[19] Li, R., Corripio, A.B., Henson, M.A., Kurtz, M.J. (2004): On-line state and parameter estimation of EPDM polymerization reactors using a hierarchical extended Kalman filter. – Journal of Process Control 14(8): 837-852.
[20] McAfee, T., Leonardi, N., Montgomery, R., Siqueira, J., Zekoski, T., Drenski, M.F., Reed, W.F. (2016): Automatic control of polymer molecular weight during synthesis. – Macromolecules 49(19): 7170-7183.
[21] McKeen, L.W. (2014): The effect of temperature and other factors on plastics and elastomers. – William Andrew 752p.
[22] Narwekar, K., Shah, V.A. (2020): Temperature control using sliding mode control: an experimental approach. – In Information and Communication Technology for Sustainable Development: Proceedings of ICT4SD 2018, Springer Singapore 8p.
[23] Park, M.J., Hur, S.M., Rhee, H.K. (2002): Online estimation and control of polymer quality in a copolymerization reactor. – AIChE Journal 48(5): 1013-1021.
[24] Rahman, A.F.N.A., Spurgeon, S.K., Yan, X.G. (2010): Sliding mode observer based control for a continuous fermentation process. – In UKACC International Conference on Control 2010, IET 6p.
[25] Richards, J.R., Congalidis, J.P. (2006): Measurement and control of polymerization reactors. – Computers & Chemical Engineering 30(10-12): 1447-1463.

[26] Salas, S.D., Ghadipasha, N., Zhu, W., Mcafee, T., Zekoski, T., Reed, W.F., Romagnoli, J.A. (2018): Framework design for weight-average molecular weight control in semi-batch polymerization. – Control Engineering Practice 78: 12-23.
[27] Sinha, A., Mishra, R.K. (2018): Control of a nonlinear continuous stirred tank reactor via event triggered sliding modes. – Chemical Engineering Science 187: 52-59.
[28] Uçak, K., Öke Günel, G. (2020): An adaptive sliding mode controller based on online support vector regression for nonlinear systems. – Soft Computing 24(6): 4623-4643.
[29] Ullah, S., Mehmood, A., Khan, Q., Rehman, S., Iqbal, J. (2020): Robust integral sliding mode control design for stability enhancement of under-actuated quadcopter. – International Journal of Control, Automation and Systems 18: 1671-1678.
[30] Wang, Y., Chen, J., Yan, F., Zhu, K., Chen, B. (2019): Adaptive super-twisting fractional-order nonsingular terminal sliding mode control of cable-driven manipulators. – ISA Transactions 86: 163-180.
[31] Wu, H., Chen, Y., Wang, J. (2017): Model-free output feedback control of molecular weight distribution. – In 2017 6th Data Driven Control and Learning Systems (DDCLS), IEEE 6p.
[32] Yuan, P., Zhang, B., Mao, Z. (2017): A self-tuning control method for Wiener nonlinear systems and its application to process control problems. – Chinese Journal of Chemical Engineering 25(2): 193-201.